

# Fractionally Quantized Berry Phase, Adiabatic Continuation, and Edge States

Toshikaze Kariyado\* and Yasuhiro Hatsugai†  
 Division of Physics, Faculty of Pure and Applied Sciences,  
 University of Tsukuba, Tsukuba, Ibaraki 305-8571, Japan  
 (Dated: March 1, 2022)

Symmetry protected quantization of the Berry phase is discussed in relation to edge states. Assuming an existence of some adiabatic process which protects quantization of the Berry phase, non trivial Berry phase  $\gamma = \pm 2\pi\rho$  ( $\rho$  is a local filling of particles) for the bulk suggests appearance of edge states with boundaries. We have applied this generic consideration for Bloch states of some two dimensional model with massless Dirac fermions where  $\gamma = \pm\pi/2$  implies the edge states. Entanglement entropy is evaluated for the models and its relation to the bulk–edge correspondence of Dirac fermions is discussed as well.

PACS numbers: 73.20.-r, 03.65.Vf, 03.65.Ud

Characterization of phases is one of the main targets of condensed matter physics. As for a description of physical states, roles of boundary conditions have been assumed secondary. It is true when one considers classical order using a order parameter in the thermodynamic limit, since the dimensions of boundaries are less than the bulk dimension. In topological phases characterized by absence of local order parameters[1], the situation is different. In contrast to the symmetry broken phases with low energy excitations as the Nambu-Goldstone boson, the ground state of the topological phase is mostly gapped as a bulk. With boundaries or impurities, however, there exist low energy excitations only near such geometrical disturbance[2–8]. This edge states/boundary states characterize the topological phases. For instance, the number of edge states of quantum Hall system can be predicted by Chern number defined with the bulk Hamiltonian[9], and this is known as the bulk–edge correspondence[10, 11]. Another example is  $Z_2$  topological insulator[12, 13] that is characterized by nontrivial  $Z_2$  topological number and exhibits novel surface states.

In order to analyze the origin of edge states, an adiabatic continuation is useful. Assuming a modification of the gapped ground state of the bulk to a simple state without gap closing, one may reduce the topological properties of the physical system to those of the simple one. When the reduced system is composed of independent clusters, edge states can be understood as dangling states appearing as a result of breaking a cluster at the generic edges[7, 14]. On the other hand, if the boundary does not break a cluster, i.e., the boundary is in between two adjoined clusters, there is no obvious reason to have edge states. The adiabatic continuation is more powerful when it is combined with topological quantities defined by the Berry connection [15–18] using gauge twists as parameters. Among the topological quantities, the Chern numbers are quantized by its definition but the Berry phase and its generalizations are quantized with the help of some symmetries[14, 19, 20]. When such symmetries present, the Berry phase based argument is robust against adiabatic continuation, as far as the symmetry is kept during the adiabatic continuation. Furthermore, the entanglement entropy is also useful to characterize topological properties and edge states[21–25].

In this paper, we first give general arguments for characterizing a gapped and short-range entangled state using an adiabatic continuation and the Berry phase. A natural interpretation of the bulk–edge correspondence in that general framework is also given. Then to demonstrate the general idea, we introduce a model having Dirac cones in its bulk energy dispersion as an example where an unusual type of the quantization of the Berry phase, the quantization into  $\pm\pi/2$ , or fractional quantization is used to demonstrate the bulk–edge correspondence of the Dirac fermions.

Let us start our discussion from a generic lattice model of spinless fermions by a hamiltonian with an adiabatic parameter  $\lambda$  (extension with spins or for systems with  $U(1)$  gauge invariance is straightforward)

$$H(\lambda) = H_{E,E} + H_{L,L} + \lambda H_{L,E}$$

$$H_{\alpha\beta} = \sum_{i \in \alpha, j \in \beta} (c_i^\dagger t_{ij} c_j + h.c. + V_{ij} n_i n_j), \quad \alpha, \beta = L, E$$

where  $n_i = c_i^\dagger c_i$  and the system is divided into two parts  $L$  and  $E$ . The parameter  $\lambda$  is a coupling between them (Fig. 1). It is invariant for a  $U(1)$  gauge transformation  $H \rightarrow H' = H$  where  $c_i \rightarrow c'_i = \Omega_i c_i$  and  $t_{ij} \rightarrow t'_{ij} = \Omega_i t_{ij} \Omega_j^{-1}$ , ( $|\Omega_i| = 1$ ). We assume the manybody ground state  $|G(\lambda)\rangle$  of  $H(\lambda)$  is always gapped for  $0 \leq \lambda \leq 1$ . The physical ground state  $|G(1)\rangle$  is adiabatically connected to the decoupled ground state  $|G(0)\rangle$  written as

$$|G(0)\rangle = \sum_{i_1 i_2 \dots \in L} \psi_{i_1 i_2 \dots}^L c_{i_1}^\dagger c_{i_2}^\dagger \dots \sum_{j_1 j_2 \dots \in E} \psi_{j_1 j_2 \dots}^E c_{j_1}^\dagger c_{j_2}^\dagger \dots |0\rangle. \quad (1)$$

It implies that the ground state  $|G(1)\rangle$  is short-range entangled, that is, the ground state is composed of local quantum objects. Typical such examples are the Haldane phase of the spin 1 chain and the valence bond solid states[18, 26, 27]. To characterize this short-range entanglement, let us define a Berry phase  $\gamma$  by introducing a gauge twist  $\omega_\ell = e^{i\theta}$ , ( $0 \leq \theta \leq 2\pi$ ) at some sites  $\ell$ 's inside the local object  $L$  ( $\ell$ 's can be multiple sites). This twist dependence is given by the local hamiltonian  $H_{L,L}(\omega_\ell)$  where the hopping  $t_{i\ell}$  connecting the sites  $\ell$ 's and the remained sites  $i$ 's inside the local object  $L$  are replaced by  $t_{i\ell}\omega_\ell$ . Note that this gauge twist does not affect any coupling

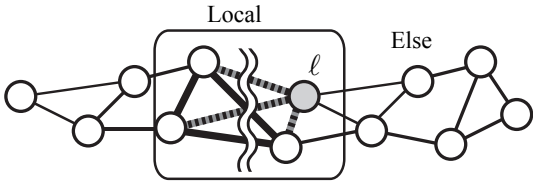


FIG. 1. General idea of the Berry phases and edge states. Hopping of the thick dotted lines are modified. When the local object  $L$  is decoupled (only the hopping on the thick lines is non zero), this gauge twists are gauged away.

in  $H_{L,E}$ . Then the Berry phase defined below characterizes the locality of the gapped phase

$$i\gamma = \int \langle G|dG \rangle = \int_0^{2\pi} d\theta \langle G|\partial_\theta G \rangle \quad \text{mod } 2\pi. \quad (2)$$

As for the decoupled case, this  $\gamma$  is easily evaluated as  $\gamma = 2\pi\bar{\rho}$  where  $\bar{\rho} = \sum_\ell (2\pi)^{-1} \int_0^{2\pi} d\theta \langle G(0)|n_\ell|G(0) \rangle$  is sum of an averaged filling of the fermion at the site  $\ell$  since the gauge twist  $\omega_\ell$  is gauged out by the gauge transformation[28]. If there exists some symmetry (such as the chiral symmetry, reflection, time reversal) to guarantee the quantization of the Berry phase  $\gamma$ , this Berry phase is an adiabatic invariant and used for a topological order parameter at the physical point  $\lambda = 1$ . We have many successful examples for such situations[18, 29–31]. Even if such a symmetry is absent, we may still expect that substantially large value of  $\gamma$  implies an existence of the short range entanglement. That is, the Berry phase  $\gamma$  can be a good topological order parameter.

For the gapped phase that can be well described by a collection of local objects  $L$ , a finite  $\gamma$  suggests appearance of edge states when the boundary is on the gauge twisted bonds. In the decoupled limit, such boundary breaks a local object and broken pieces appear as edge states[32]. Even for a finite coupling, the edge states can be still localized with the symmetry protection, since the Berry phase  $\gamma$  is an adiabatic invariant and the locality of the ground state retains as well. This general idea can be applied for several systems. Application is not limited to one-dimensional systems and applicable to higher dimensions. When the system is free of manybody interactions, momenta parallel to a given edge (or surface) are regarded as parameters determining effective one-dimensional model. One of such important examples is a zero mode edge state at the zigzag boundary of graphene which is characterized by the Berry phase in the effective one-dimensional model [14, 33, 34]. Quantization of the Berry phase  $\gamma/\pi \in \mathbb{Z}$  is well known today but here in this paper, we demonstrate  $\gamma = \pm\pi/2$ , i.e., a fractional quantization of  $\gamma$  is also useful for the bulk-edge correspondence of the Dirac fermions.

The locality of the gapped ground state is also reflected in the entanglement entropy. In the  $\lambda = 0$  limit, there is no need to consider the entanglement between  $L$  and  $E$ . Then, we divide  $L$  into two parts  $L_A$  and  $L_B$  (corresponds to breaking

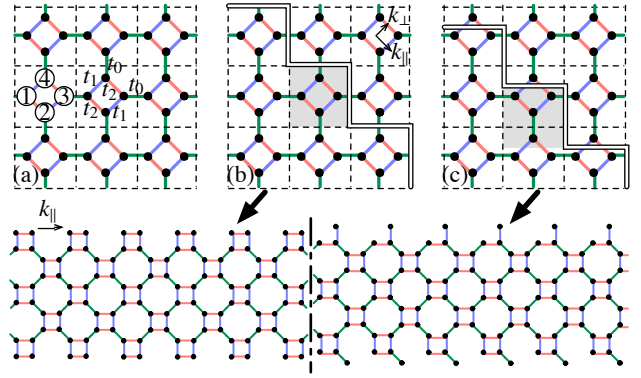


FIG. 2. (a) Definitions of transfer integrals. Namings of sublattices are also shown. (b) and (c) Definitions of type 1 and type 2 edges. Shaded regions are corresponding unit cells. Examples of ribbons for edge spectrum calculations are shown in lower panels.

the local object  $L$ ), and calculate the entanglement entropy by tracing out the information in  $L_B$ . For the noninteracting case with one fermion in  $L_A$  or one lattice site in  $L_A$ , the entanglement entropy is readily evaluated as

$$S = -[\bar{\rho} \log \bar{\rho} + (1 - \bar{\rho}) \log(1 - \bar{\rho})], \quad (3)$$

where  $\bar{\rho}$  is the fermion filling in  $L_A$ . Just as in the case of the Berry phase, it is determined from  $\bar{\rho}$  only, i.e., there is a solid relation between the Berry phase and the entanglement entropy in some limit[21].  $S$  in Eq. (3) takes maximum when  $\bar{\rho} = 0.5$ , which corresponds to  $\gamma = \pi$ . Although Eq. (3) is for a specific limit, one may expect strong correlation between the Berry phase and the entanglement entropy through edge states in general[30].

As an example to describe general ideas explained above, we introduce a spinless fermionic tight-binding model having four sublattices in a unit cell. [See Fig. 2(a).] We define three kinds of transfer integrals,  $t_0$ ,  $t_1$ , and  $t_2$  as in Fig. 2(a), and set  $t_0 = 1.0$ ,  $t_1 = 0.5$ , and  $t_2 = 1.5$  throughout this paper. Properties of the very similar model have been addressed in Ref. 35 very recently, and thus, we concentrate on the Berry phase and its fractional quantization in this paper. For the edge state characterization, we consider two kinds of edge shapes named as type 1 and type 2. [See Figs. 2(b).] In order to treat a two-dimensional model, we introduce momenta parallel ( $k_{\parallel}$ ) and perpendicular ( $k_{\perp}$ ) to the edge whose directions are shown in Fig. 2(b), with  $k_{\perp}$  acting as a parameter determining an effective one-dimensional model. In the present case, the gauge twist  $\omega_\ell = e^{i\theta}$  can be regarded as a twisted boundary condition, and the integration over  $\theta$  can be mapped to the integration over  $k_{\perp}$ . Then, the Berry phase Eq. (2) is given by the Zak phase[36]

$$i\gamma(k_{\parallel}) = \sum_{n \in \text{filled}} \int_{-\pi}^{\pi} dk_{\perp} \langle u_{nk_{\parallel}, k_{\perp}} | \partial_{k_{\perp}} | u_{nk_{\perp}, k_{\parallel}} \rangle, \quad (4)$$

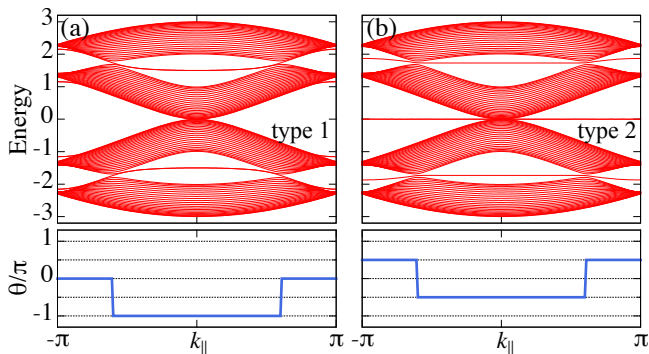


FIG. 3. Energy spectra and Berry phases for quarter filling for type 1 (a) and type 2 (b) edges.

and we use this expression for computational convenience. Here,  $k_{\perp}$  is properly scaled so that the Bloch wave function  $|u_{nk_{\perp}, k_{\parallel}}\rangle$  has periodicity  $2\pi$  in  $k_{\perp}$ . Note that a unit cell convention is directly related to  $\gamma(k_{\parallel})$ . For each boundary shape, we set a unit cell so that the given boundary lies in between two neighboring unit cells[20] to use the Berry phase  $\gamma(k_{\parallel})$  to discuss the edge states. [See shaded regions in Figs. 2(b) and (c).] We employ the technique in Refs. 37 and 28 for the Berry phase calculations. Edge spectrum is calculated with ribbon geometry like those in the lower panels of Fig. 2, though the actual calculations are performed on much wider ribbons. In order to discuss the fractional quantization, we focus on the quarter filling case, the case of one fermion per a unit cell, throughout this paper.

Figure 3 shows the edge spectra (upper panels) and the Berry phases (lower panels) for the type 1 (a) and type 2 (b) edges. As we handle the quarter filling case, we should focus on the lowest band and the gap just above it. For the given parameter set, Dirac cones appear between the lowest and second lowest bands in the bulk energy dispersion. Consequently, the bulk continuum, the region filled with bands with bulk nature, touches at two points, which are projected Dirac cones. For the type 1 edge, the Berry phase is quantized into 0 and  $\pi$ . On the other hand, for the type 2 edge, the Berry phase is quantized into  $\pm\pi/2$ , i.e., the fractional quantization is really achieved. As we have noted, the Berry phase is related to the site resolved filling  $\bar{\rho}$ . Here, the sublattice and  $k_{\parallel}$  resolved filling  $\rho_a(k_{\parallel})$  plays a role of  $\bar{\rho}$ . For the present model, the time reversal symmetry gives  $\rho_a(-k_{\parallel}) = \rho_a(k_{\parallel})$ , the inversion symmetry gives  $\rho_1(-k_{\parallel}) = \rho_3(k_{\parallel})$  and  $\rho_2(-k_{\parallel}) = \rho_4(k_{\parallel})$ , and the mirror symmetry gives  $\rho_1(-k_{\parallel}) = \rho_2(k_{\parallel})$  and  $\rho_3(-k_{\parallel}) = \rho_4(k_{\parallel})$ . In addition,  $\sum_a \rho_a(k_{\parallel}) = 1$  for the quarter filling. Combining these relations, we finally obtain the relation  $\rho_a(k_{\parallel}) = 1/4$ , which leads to the fractional quantization of the Berry phase into  $\pm\pi/2$ . As this derivation shows, the  $\pm\pi/2$  quantization is a kind of symmetry protection by crystal symmetries.

For the type 1 edge, an edge state distinct from the bulk continuum is existing as they connect two projected Dirac cones. In the region with the edge states,  $\gamma(k_{\parallel})$  takes a value of  $\pi$

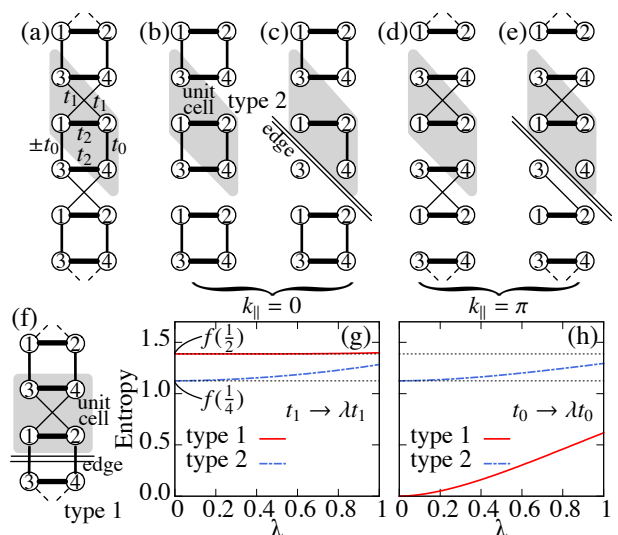


FIG. 4. (a) One dimensional model for a fixed  $k_{\parallel}$ . For the transfer integral indicated as  $\pm t_0$ , take  $+t_0$  ( $-t_0$ ) for  $k_{\parallel} = 0$  ( $\pi$ ). (b) and (d) Adiabatically continued models. (c) and (e) Adiabatically continued model after edge introduction. (b) and (c) are for  $k_{\parallel} = 0$ , while (d) and (e) are for  $k_{\parallel} = \pi$ , respectively. (g) and (h) Entanglement entropy for  $k_{\parallel} = 0$  (g) and  $k_{\parallel} = \pi$  (h). A function  $f(x) = -2[x \log x + (1-x) \log(1-x)]$ .

( $-\pi$  is equivalent to  $\pi$ ). Existence/absence of the edge state are switched at the gap closing point, which is consistent with  $\pi$ -jump in  $\gamma(k_{\parallel})$ [20]. In this case, the edge states are doubly degenerate and they are localized at left and right boundaries, respectively. In contrast, edge states appearing for the type 2 edge, for which  $\pm\pi/2$  quantization takes place, are different. There appears only one nondegenerate edge state through the entire edge Brillouin zone. In this case, the spacial position of the edge states are switched at the projected Dirac cone. Namely, the edge state near  $k_{\parallel} = 0$  lives on the edge at the one side of the ribbon, say the left edge, while the one near  $k_{\parallel} = \pi$  lives on the edge at the other side.

Here, we apply adiabatic continuation focusing on the effective one-dimensional model for  $k_{\parallel} = 0$  and  $\pi$ . Schematically, this one-dimensional model is illustrated in Fig. 4(a), in which a plus (minus) sign should be taken for the transfer integral denoted as  $\pm t_0$  for  $k_{\parallel} = 0$  ( $k_{\parallel} = \pi$ ). The type 1 and 2 edges and the corresponding unit cell conventions in the effective one-dimensional model are indicated as doubled lines and shaded regions in Fig. 4. For  $k_{\parallel} = 0$ , the model can be adiabatically connected, i.e., smoothly transformed without closing the gap between the lowest and second lowest bands, to the model in Fig. 4(b) by replacing  $t_1$  by  $\lambda t_1$  and reducing  $\lambda$  from 1 to 0 gradually. Note that the model in  $\lambda \rightarrow 0$  limit is composed of decoupled clusters, or local objects, and this operation maintains the symmetry of the model and the Berry phase quantization. For  $k_{\parallel} = \pi$ , a different adiabatic continuation must be applied to keep the gap, namely, we should replace  $t_0$  by  $\lambda t_0$  and take  $\lambda \rightarrow 0$  limit. This operation results

in a model in Fig. 4(d).

Next, we explicitly show that edge states are induced by breaking local objects. For  $k_{\parallel} = 0$ , the energy levels in the  $\lambda \rightarrow 0$  limit are  $t_2 + t_0$ ,  $t_2 - t_0$ ,  $-t_2 + t_0$ , and  $-t_2 - t_0$ . Then, if the type 2 edge is introduced here, it breaks the local object at the edge as Fig. 4(c), and modifies the energy levels to  $\pm(t_2^2 + t_0^2)^{1/2}$  and 0 (doubly degenerate). Since  $-t_2 - t_0 < -(t_2^2 + t_0^2)^{1/2} < -t_2 + t_0$ , the state with energy  $-(t_2^2 + t_0^2)^{1/2}$  appear as an ingap edge state in Fig. 4(b) near  $k_{\parallel} = 0$ . The wave function for this ingap state has its weight only in the *upper* side of the doubled line in Fig. 4(c). In the exactly same way, the origin of the edge state near  $k_{\parallel} = \pi$  in Fig. 3(b) can be identified, but due to the difference in the adapted adiabatic continuation, the wave function for the ingap state has its weight only in the *lower* side of the doubled line in Fig. 4(e), which is opposite from the case of  $k_{\parallel} = 0$ .

Figure 4 also shows the entanglement entropy for  $k_{\parallel} = 0$  and  $\pi$ . In practice, the entanglement entropy is numerically calculated using the formula based on the correlation function  $\langle c_i^{\dagger} c_j \rangle$ [38], and arranging the effective one-dimensional model in a closed circle shape and inserting two cuts to perform bipartition. Here, two cuts are required to divide a closed circle into two parts, and two local objects (in the decoupled limit) are broken in this procedure. We consider two kinds of cutting shapes corresponding to the type 1 and 2 boundary. In order to see effects of the adiabatic continuation, we plot  $\lambda$  dependence of the entanglement entropy for  $k_{\parallel} = 0$  [Fig. 4(g)] and  $\pi$  [Fig. 4(h)]. For  $k_{\parallel} = 0$ , the entanglement entropy is finite in  $\lambda \rightarrow 0$  limit for both of the type 1 and 2 edges, which nicely fits the observation of the edge states for  $k_{\parallel} = 0$  for both types of edges in Fig. 3. On the other hand, for  $k_{\parallel} = \pi$ , the entanglement entropy in  $\lambda \rightarrow 0$  limit is finite only for the type 2 edge, and zero for the type 1 edge. Again, this result fits appearance (absence) of the edge state for  $k_{\parallel} = \pi$  for the type 1 (type 2) edge in Fig. 3. Figs. 4(g) and 4(h) also indicate that the entanglement entropy in  $\lambda \rightarrow 0$  limit is really derived by the formula Eq. (3) with extra factor of two coming from our procedure to make bipartition in which two local objects are broken.

To summarize, we develop a general theory to characterize a gapped and short-range entangled state on the basis of adiabatic continuation and the Berry phase. There, we give a natural interpretation of the bulk–edge correspondence with the idea of a broken local object. The relation between the Berry phase and the entanglement entropy in a specific limit is also pointed out. In the latter half, the general ideas are tested in a model with Dirac cones. We find a new type of the Berry phase quantization, the quantization into  $\pm\pi/2$  in the introduced model. It is also shown that the new type of the quantization modifies the way of edge state emergence from the case of usual  $0/\pi$  quantization.

This work is partly supported by Grants-in-Aid for Scientific Research, No.26247064, No.23340112, No.25610101, and No.23540460 from JSPS.

\* kariyado@rhodia.ph.tsukuba.ac.jp

† hatsugai@rhodia.ph.tsukuba.ac.jp

- [1] X. G. Wen, Phys. Rev. B **40**, 7387 (1989).
- [2] B. I. Halperin, Phys. Rev. B **25**, 2185 (1982).
- [3] W. P. Su, J. R. Schrieffer, and A. J. Heeger, Phys. Rev. Lett. **42**, 1698 (1979).
- [4] C.-R. Hu, Phys. Rev. Lett. **72**, 1526 (1994).
- [5] Y. Tanaka and S. Kashiwaya, Phys. Rev. Lett. **74**, 3451 (1995).
- [6] M. Fujita, K. Wakabayashi, K. Nakada, and K. Kusakabe, J. Phys. Soc. Jpn. **65**, 1920 (1996).
- [7] A. Y. Kitaev, Physics-Uspekhi **44**, 131 (2001).
- [8] Volovik, *The Universe in a Helium Droplet* (Clarendon Press, Oxford, 2003).
- [9] D. J. Thouless, M. Kohmoto, M. P. Nightingale, and M. den Nijs, Phys. Rev. Lett. **49**, 405 (1982).
- [10] Y. Hatsugai, Phys. Rev. Lett. **71**, 3697 (1993).
- [11] Y. Hatsugai, Phys. Rev. B **48**, 11851 (1993).
- [12] M. Z. Hasan and C. L. Kane, Rev. Mod. Phys. **82**, 3045 (2010).
- [13] X.-L. Qi and S.-C. Zhang, Rev. Mod. Phys. **83**, 1057 (2011).
- [14] S. Ryu and Y. Hatsugai, Phys. Rev. Lett. **89**, 077002 (2002).
- [15] M. V. Berry, Proc. R. Soc. A **392**, 45 (1984).
- [16] Y. Hatsugai, J. Phys. Soc. Jpn. **73**, 2604 (2004).
- [17] Y. Hatsugai, J. Phys. Soc. Jpn. **74**, 1374 (2005).
- [18] Y. Hatsugai, J. Phys. Soc. Jpn. **75**, 123601 (2006).
- [19] Y. Hatsugai, New J. Phys. **12**, 065004 (2010).
- [20] T. Kariyado and Y. Hatsugai, Phys. Rev. B **88**, 245126 (2013).
- [21] S. Ryu and Y. Hatsugai, Phys. Rev. B **73**, 245115 (2006).
- [22] M. Arikawa, S. Tanaya, I. Maruyama, and Y. Hatsugai, Phys. Rev. B **79**, 205107 (2009).
- [23] M.-C. Chung, Y.-H. Jhu, P. Chen, and S. Yip, Europhys. Lett. **95**, 27003 (2011).
- [24] T. L. Hughes, E. Prodan, and B. A. Bernevig, Phys. Rev. B **83**, 245132 (2011).
- [25] A. Chandran, M. Hermanns, N. Regnault, and B. A. Bernevig, Phys. Rev. B **84**, 205136 (2011).
- [26] X. Chen, Z.-C. Gu, and X.-G. Wen, Phys. Rev. B **82**, 155138 (2010).
- [27] F. Pollmann, E. Berg, A. M. Turner, and M. Oshikawa, Phys. Rev. B **85**, 075125 (2012).
- [28] T. Hirano, H. Katsura, and Y. Hatsugai, Phys. Rev. B **78**, 054431 (2008).
- [29] I. Maruyama and Y. Hatsugai, J. Phys. Soc. Jpn. **76**, 113601 (2007).
- [30] T. Hirano, H. Katsura, and Y. Hatsugai, Phys. Rev. B **77**, 094431 (2008).
- [31] I. Maruyama, T. Hirano, and Y. Hatsugai, Phys. Rev. B **79**, 115107 (2009).
- [32] When the boundary allows multiple edge states within a finite region, residual interaction among the edge states can be effective which makes the edge states gapped.
- [33] Y. Hatsugai, Solid State Commun. **149**, 1061 (2009).
- [34] P. Delplace, D. Ullmo, and G. Montambaux, Phys. Rev. B **84**, 195452 (2011).
- [35] Y. Yamashita, M. Tomura, Y. Yanagi, and K. Ueda, Phys. Rev. B **88**, 195104 (2013).
- [36] J. Zak, Phys. Rev. Lett. **62**, 2747 (1989).
- [37] R. D. King-Smith and D. Vanderbilt, Phys. Rev. B **47**, 1651 (1993).
- [38] I. Peschel and V. Eisler, J. Phys. A: Math. Theor. **42**, 504003 (2009).